

CW lasing in Yb^{3+} : GGG crystals pumped at 0.925 μm

A.M. Belovolov, M.I. Belovolov, E.M. Dianov, V.V. Dudin, M.I. Timoshechkin

Abstract. Single-mode cw lasing was obtained for the first time in Yb^{3+} : GGG crystals at room temperature at 1.030 and 1.037 μm upon pumping Yb^{3+} ions by a 0.925- μm neodymium-doped fibre laser. Lasing was observed at the transitions between the lower Stark sublevel of the ${}^2\text{F}_{5/2}$ level and the upper Stark sublevels of the ${}^2\text{F}_{7/2}$ ground state of Yb^{3+} ions. The study of lasing characteristic showed that lasing occurs according to the four-level scheme. The lasing threshold with respect to the absorbed power was 85 mW and the slope lasing efficiency was 20 %. Upon 1.7-W pumping, the output power of 310 mW was achieved with the output resonator mirror with the transmission coefficient of 1 %. The effective cross section of the lasing transition was $0.9 \times 10^{-20} \text{ cm}^2$.

Keywords: single-mode Yb^{3+} : GGG laser, four-level lasing scheme, emission spectrum.

1. Introduction

At present considerable attention is being given to the study of Yb^{3+} -doped active media for solid-state lasers. The advantages of ytterbium-doped media are a simple energy level diagram of Yb^{3+} ions, which excludes cross relaxation, and a large laser linewidth attractive for generating ultrashort laser pulses [1–5]. In addition, the emission wavelength of ytterbium lasers is close to the pump wavelength, which reduces heat release in the active medium and substantially improves the thermal regime of these lasers compared to neodymium lasers [1–5]. Lasing in Yb^{3+} ions in Nd : Yb : GGG crystals was first obtained at 1.0232 μm at temperature 77 K upon flashlamp pumping in 1975 [6]. Since then, despite progress in the development of diode laser pump systems, lasing in Yb^{3+} : GGG lasers has not been achieved, and the outlook for the development and application of such lasers is still uncertain. Numerous attempts to obtain cw lasing upon pumping by diode lasers or diode laser arrays have not given yet positive results, and

low lasing thresholds have not been achieved. This suggests that Yb^{3+} : GGG crystals have a number of specific features related to their pumping and pump energy transfer and are very sensitive to the geometry of laser experiments.

Single-mode cw lasing at 1.037 μm in Yb^{3+} : GGG crystals pumped by a Ti : sapphire laser at 0.944 and 0.97 μm was reported in [7, 8]. The aim of our paper is to continue investigations of lasing in these crystals pumped at a wavelength of 0.925 μm , which can be realised upon diode pumping.

2. Experimental results and discussion

Figure 1 shows the scheme of the experimental setup for studying lasing in Yb^{3+} : GGG crystals. The crystals were pumped by a 0.925- μm , 2.2-W cw neodymium-doped fibre laser developed in [9].

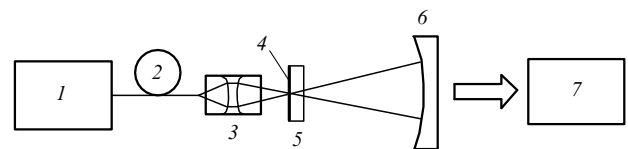


Figure 1. Scheme of the experimental setup for studying lasing in Yb^{3+} : GGG crystals: (1) 0.925- μm , 2.2-W neodymium-doped fibre laser [9]; (2) single-mode fibre; (3) two-lens 1:2 C230220P objective; (4) input flat mirror of the resonator (with high transmission at 0.925 μm and high reflection at 1.03–1.04 μm); (5) Yb^{3+} : GGG active element; (6) output spherical mirror of the resonator (with the transmission coefficient $T = 1\%$ at 1.04 μm , high reflection coefficient at 0.925 μm , and radius of curvature $R = 5$ cm); (7) AQ-6310 optical spectrum analyser or power meter.

Figure 2 presents the absorption and luminescence spectra of Yb^{3+} : GGG crystals with the indicated wavelengths of electronic transitions between the corresponding Stark sublevels of the ${}^2\text{F}_{7/2}$ ground state and the ${}^2\text{F}_{5/2}$ excited state used in this paper and [7]. The mode-field diameter of the output single-mode fibre of the neodymium laser was 8.0 μm . Pump radiation was focused with a long-focus 1:2 C230220P-B objective (THOR-LABS) which provided an increase in the beam waist size and ensured good focusing over the entire length of the crystal. The laser had a semiconfocal resonator consisting of a flat mirror on the active crystal and the output spherical mirror with the radius of curvature $R = 5$ cm and the transmission coefficient $T = 1\%$ in the range from 1.03 to 1.06 μm . The active

A.M. Belovolov, M.I. Belovolov, E.M. Dianov, V.V. Dudin Fiber Optics Research Center, Russian Academy of Sciences, ul. Vavilova 38, 119991 Moscow, Russia; e-mail: bmi@fo.gpi.ru;

M.I. Timoshechkin A.M. Prokhorov General Physics Institute, Russian Academy of Sciences, ul. Vavilova 38, 119991 Moscow, Russia

Received 12 April 2006

Kvantovaya Elektronika 36 (7) 587–590 (2006)

Translated by M.N. Sapozhnikov

crystal of length 1 mm was doped with Yb^{3+} ions at the atomic concentration 17%. The $\text{Yb}^{3+}:\text{GGG}$ crystals contained uncontrollable impurities of rare-earth Ho^{3+} ions at the atomic concentration $10^{-3}\%$ – $10^{-2}\%$, whose role was noticeable, the excited-state lifetime τ of Yb^{3+} ions being decreased in their presence down to ~ 0.827 ms compared to the expected lifetime $\tau_0 \approx 1.05$ ms for pure crystals. The rate of stationary quenching of excited Yb^{3+} ions by uncontrolled impurities determined from τ_0 and τ was $W = \tau^{-1} - \tau_0^{-1} = 257 \text{ s}^{-1}$.

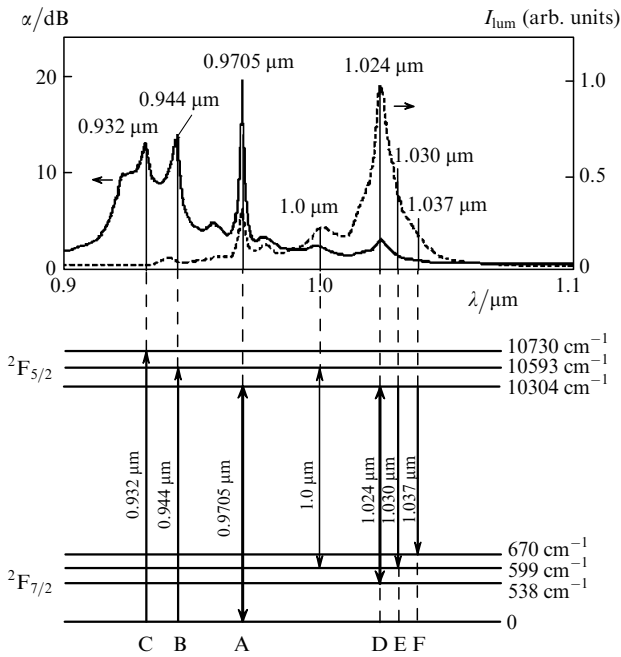


Figure 2. Absorption $\alpha(\lambda)$ and luminescence $I_{\text{lum}}(\lambda)$ spectra of $\text{Yb}^{3+}:\text{GGG}$ crystals (17% of Yb^{3+} , the sample thickness is $l = 2.2$ mm) at 300 K and main electronic transitions in the energy level diagram of Yb^{3+} ions. The emission transitions at 1.030 and 1.037 μm are determined in this paper from lasing experiments.

The emission spectra of the $\text{Yb}^{3+}:\text{GGG}$ laser pumped by a 0.925- μm neodymium laser are presented in Figs 3 and 4. As the absorbed pump power was increased from the threshold value (85 mW) up to 0.5 W, one laser line was observed at 1.037 μm , which corresponded to the lasing transition from the lower Stark level of the $^2F_{5/2}$ state to the upper Stark level of the $^2F_{7/2}$ ground state. We observed earlier cw lasing at the $^2F_{5/2} - ^2F_{7/2}$ transition at 1.037 μm in experiments with pumping by a Ti:sapphire laser [7, 8]. These data gave the energy (670 cm^{-1}) of the upper Stark level, which cannot be determined sufficiently accurately from the absorption and luminescence spectra in Fig. 2.

We found in this paper that, as the pump power was increased up to 1.7 W, lasing occurred simultaneously at 1.037 and 1.030 μm . Figure 4 shows that both these lines have the same width ~ 2 nm, and the spontaneous emission background is three orders of magnitude (-30 dB) is lower than the 1.037- μm line intensity. We assigned the 1.030- μm line to the transition from the 10304- cm^{-1} excited state to the second 599- cm^{-1} Stark level of the $^2F_{7/2}$ ground state, which also cannot be determined accurately due to the inhomogeneous broadening of the corresponding spectral bands caused by the electron–phonon interaction. Thus, by

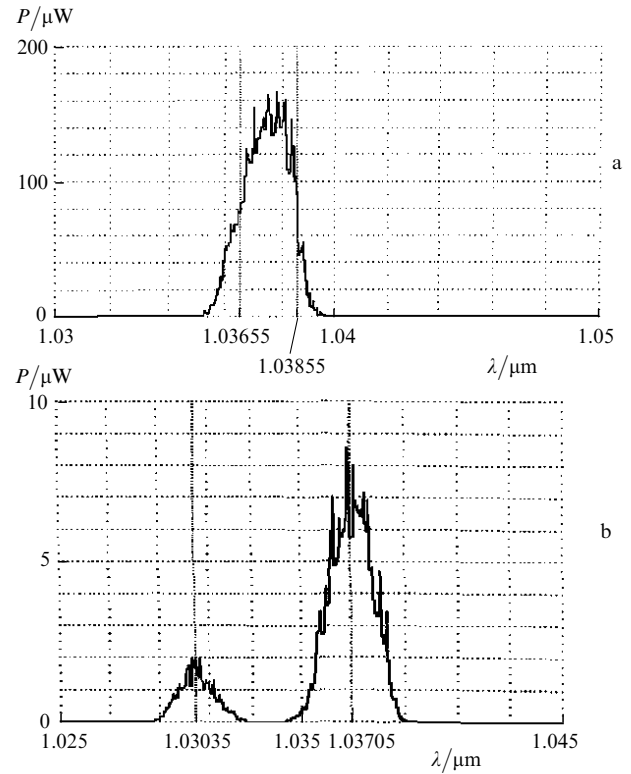


Figure 3. Emission spectra of the cw $\text{Yb}^{3+}:\text{GGG}$ laser (linear scale) for pump powers 0.5 (a) and 1.7 W (b).

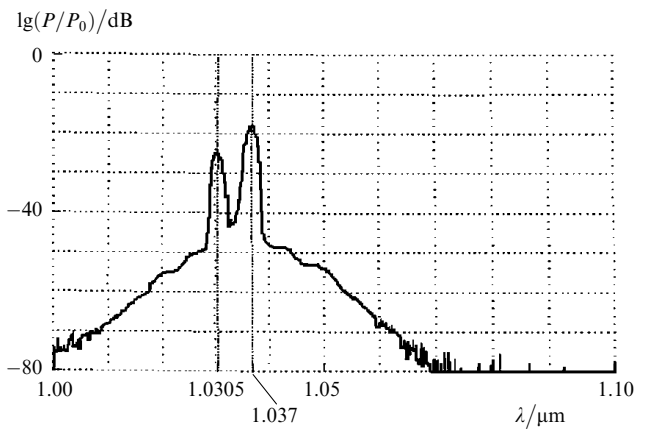


Figure 4. The 1.030- μm and 1.037- μm lines of the $\text{Yb}^{3+}:\text{GGG}$ laser pumped by a 0.925- μm , 1.7-W neodymium-doped fibre laser (logarithmic scale, spontaneous emission level is -30 dB).

using the wavelengths 1.030 and 1.037 μm of the laser lines observed in our experiments, we refined the energies of two Stark sublevels of the $^2F_{7/2}$ multiplet of Yb^{3+} ions in $\text{Yb}^{3+}:\text{GGG}$ crystals at room temperature, which proved to be equal to 599 and 670 cm^{-1} , respectively.

Figure 5 shows the dependence of the output power of the $\text{Yb}^{3+}:\text{GGG}$ laser on the absorbed pump power. The linearity of this dependence above the lasing threshold suggests that lasing occurs according to the four-level scheme [10]. The absorbed threshold power was $P_{\text{th}} = 85$ mW and the slope efficiency was $\eta = 20\%$. The output single-mode cw power was 310 mW for the absorbed pump power of 1.7 W.

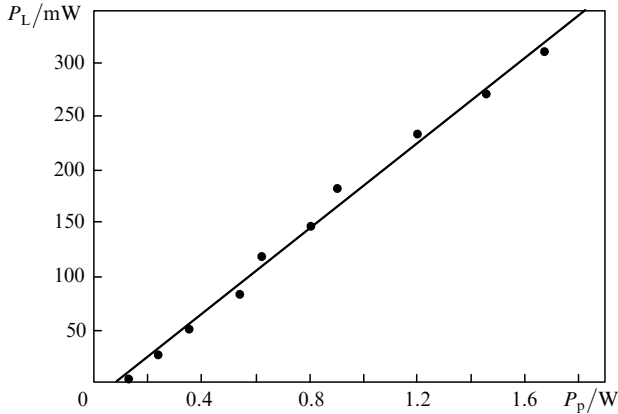


Figure 5. Dependence of the output power of the Yb³⁺:GGG laser on the absorbed pump power at 0.925 μm.

The lasing parameters were calculated from the system of balance equations for the population difference at the lasing transition and the number of photons in the resonator, similarly to the calculation performed in [10, 11]. Unlike papers [10, 11], we took into account in the calculation the quenching of the upper laser level due to the energy transfer to uncontrollable impurities and the Boltzmann distribution of the population of Stark sublevels of the $2F_{7/2}$ and $2F_{5/2}$ states. Taking into account the four-level lasing scheme, we estimated nonresonance losses δ_n in the active element from the slope efficiency [10] as

$$\delta_n \approx T \left(\frac{h\nu_L}{h\nu_p} \eta^{-1} - 1 \right) = 0.035, \quad (1)$$

where $h\nu_L/h\nu_p = \lambda_p/\lambda_L = 0.891$ is the energy ratio for laser and pump photons.

The estimate $\delta_n \approx 0.035$ coincides within the experimental error with the value $\delta_n \approx 0.0267$ that we obtained in [7] for the same active element pumped by a Ti:sapphire laser. This demonstrates a high optical quality of Yb³⁺:GGG laser crystals preserving their lasing parameters almost for a decade.

Our analysis showed that in the case of the four-level lasing scheme, the threshold pump power can be described by the expression [10]

$$P_p^{\text{th}} = \frac{\pi h\nu_p (\delta_n + T)}{4\sigma(f_1 + f_2)\tau} (w_{L0}^2 + w_{p0}^2), \quad (2)$$

where $w_{L0} = 91 \mu\text{m}$ is the radius of the mode-field distribution at the waist of the resonator caustic; $w_{p0} = 8.0 \mu\text{m}$ is the radius of the beam-pump waist; $f_1 = 0.034$ and $f_2 = 0.727$ are the Boltzmann population factors for the lower and upper laser levels, respectively [10]; and σ is the stimulated transition cross section.

By knowing the threshold power P_p^{th} and other parameters of the laser, we estimated from (2) the effective cross section σ for the lasing transition at 1.037 μm as $0.9 \times 10^{-20} \text{ cm}^2$. We present below the basic parameters of single-mode cw lasing in Yb³⁺:GGG crystals at room temperature, which can be used for the development of ytterbium lasers with the required power characteristics and for mastering and employment of high-power diode-laser pump systems.

Lasing wavelength λ_L (μm)	1.037
Laser linewidth $\Delta\lambda_L$ (nm)	2
Lifetime τ of the upper laser level (ms)	0.827
Lasing threshold P_p^{th} (mW)	85
Nonresonance losses δ_n in the active element (%)	3.5
Slope lasing efficiency η (%)	20
Cross section σ for stimulated transition at 1.037 μm (cm^2)	0.9×10^{-20}

It follows from the absorption spectrum in Fig. 2 that the wavelength range between 0.920 and 0.945 μm is most promising for diode laser pumping. The resonance absorption peak at 0.9705 μm is convenient for the first experiments on low-threshold lasing in Yb³⁺:GGG crystals pumped by a Ti:sapphire laser, which can be precisely tuned by preserving a narrow spectrum and a high directivity of the output radiation.

A special feature of our Yb³⁺:GGG crystals was the presence of impurity Ho³⁺ ions in them at the atomic concentration $10^{-3}\% - 10^{-2}\%$, which emitted intense green luminescence at $\sim 540 \text{ nm}$ (the $^5S_2, ^5F_4 - ^5I_8$ transitions in Ho³⁺ ions [8]). As a result, approximately 20% of the pump power could be spent for anti-Stokes emission. However, although the lasing transition in Yb³⁺ ions at 1.0 μm was noticeably quenched, we managed to obtain single-mode cw lasing with a comparatively low threshold by using the output resonator mirror with the transmission coefficient $T = 1\%$. Higher-power lasing in Yb³⁺:GGG crystals can be achieved by using mirrors with the optimal transmission coefficients and the optimal resonator geometry, which can be calculated with the help of the parameters of laser crystals measured in our paper.

3. Conclusions

We have obtained for the first time single-mode cw lasing at 1.030 and 1.037 μm in Yb³⁺:GGG crystals pumped at 0.925 μm at room temperature. The wavelengths of laser lines measured in experiments allowed us to refine the energies of two Stark sublevels of the $^2F_{7/2}$ ground state of Yb³⁺ ions, which are 599 and 670 cm^{-1} . The study of lasing parameters has shown that lasing occurs according to the four-level scheme. The lasing threshold was 85 mW and the slope efficiency was $\eta = 20\%$. The output power of 310 mW has been achieved upon 1.7-W pumping. The lasing parameters of Yb³⁺:GGG crystals were analysed by using the theoretical model taking into account the quenching of excited Yb³⁺ ions by uncontrollable Ho³⁺ impurities and the Boltzmann distribution of Yb³⁺ ions over Stark sublevels. The effective cross section for the 1.037-μm lasing transition and nonresonance optical losses in Yb³⁺:GGG crystals have been estimated as $\sigma = 0.9 \times 10^{-20} \text{ cm}^2$ and $\delta_n = 0.035$, respectively. The results obtained in the paper show that Yb³⁺:GGG crystals are promising for the development of cw ytterbium lasers pumped by diode lasers in the wavelength range from 0.925 to 0.945 μm.

Acknowledgements. The authors thank I.A. Bufetov for his help in lasing experiments. This work was partially supported by the Program of the President of the Russian Federation for Support of Leading Scientific Schools (Grant No. NSh-2813.2006.2).

References

1. Taira T., Saikawa J., Kobayashi T., Byer R.L. *IEEE J. Sel. Top. Quantum Electron.*, **3** (1), 100 (1997).
2. Aron A., Aka G., Viana B., et al. *Opt. Mater.*, **16** (1/2), 181 (1999).
3. Marshall C.D., Smith L.K., Beach R.J., et al. *IEEE J. Quantum Electron.*, **32**, 650 (1996).
4. Bruesselbach H.W., Smida D.S., Reeder R.A., Byren R.W. *IEEE J. Sel. Top. Quantum Electron.*, **3** (1), 105 (1997).
5. Druon F., Chenais S., Raybaut P., Balembois F., Georges P., Gaume R., Aka G., Viana B., et al. *Techn. Dig. of OSA Topical Meeting, Advanced Solid-State Lasers* (Quebec, Canada, 2002) Paper MD7.
6. Bogomolova G.A., Vylegzhanin D.N., Kaminskii A.A. *Zh. Eksp. Teor. Fiz.*, **69**, 860 (1975).
7. Belovolov M.I., Dianov E.M., Timoshechkin M.I., Barashov L.V., Belovolov A.M., Ivanov M.A., Morozov N.P., Prokhorov A.M. *Antistoksovaya lyuminesentsiya i nepreryvnaya generatsiya GGG-Yb lazera na 1.083 μm pri komnatnoi temperature* (Anti-Stokes Luminescence and CW Lasing in a Yb:GGG Crystal at Room Temperature), Preprint IOFAN, No. 1 (Moscow, 1997).
8. Belovolov M.I., Dianov E.M., Timoshechkin M.I., Barashov L.V., Belovolov A.M., Ivanov M.A., Morozov N.P., Prokhorov A.M., Timoshechkin K.M. *Proc. CLEO/Europe'96* (Hamburg, Germany, 1996) Paper CML5, p.43.
9. Bufetov I.A., Eubnov M.M., Mel'kumov M.A., Dudin V.V., Shubin A.V., Semjonov S.L., Kravtsov K.S., Gur'yanov A.N., Yashkov M.V., Dianov E.M. *Kvantovaya Elektron.*, **35**, 328 (2005) [*Quantum Electron.*, **35**, 328 (2005)].
10. Fan T.Y., Byer R.L. *IEEE J. Quantum Electron.*, **24** (6), 895 (1988).
11. Laporta P., Brussard M. *IEEE J. Quantum Electron.*, **27**, 2319 (1988).